OXFORD GENETICS

GENETICS, 2023, 225(1), iyad122
https://doi.org/10.1093/genetics/iyad122
Advance Access Publication Date: 8 July 2023
Investigation

Genetic control of the error-prone repair of a chromosomal double-strand break with 5′ overhangs in yeast

Samantha Shaltz, Sue Jinks-Robertson*

Department of Molecular Genetics and Microbiology, Duke University, Durham, NC 27710, USA

*Corresponding author: Department of Molecular Genetics and Microbiology, Duke University Medical Center, 213 Research Drive, CARL 367, Durham, NC 27710, USA. Email: sue.robertson@duke.edu

Abstract

A targeted double-strand break introduced into the genome of *Saccharomyces cerevisiae* is repaired by the relatively error-prone nonhomologous end joining (NHEJ) pathway when homologous recombination is not an option. A zinc finger nuclease cleavage site was inserted out-of-frame into the *LYS2* locus of a haploid yeast strain to study the genetic control of NHEJ when the ends contain 5′ overhangs. Repair events that destroyed the cleavage site were identified either as Lys^+ colonies on selective medium or as surviving colonies on rich medium. Junction sequences in Lys^+ events solely reflected NHEJ and were influenced by the nuclease activity of Mre11 as well as by the presence/absence of the NHEJ-specific polymerase Pol4 and the translesion-synthesis DNA polymerases Pol ζ and Pol η. Although most NHEJ events were dependent on Pol4, a 29-bp deletion with endpoints in 3-bp repeats was an exception. The Pol4-independent deletion required translesion synthesis polymerases as well as the exonuclease activity of the replicative Pol δ DNA polymerase. Survivors were equally split between NHEJ events and 1.2 or 11.7 kb deletions that reflected microhomology-mediated end joining (MMEJ). MMEJ events required the processive resection activity of Exo1/Sgs1, but there unexpectedly was no dependence on the Rad1–Rad10 endonuclease for the removal of presumptive 3′ tails. Finally, NHEJ was more efficient in nongrowing than in growing cells and was most efficient in G0 cells. These studies provide novel insights into the flexibility and complexity of error-prone DSB repair in yeast.

Keywords: DSB repair, NHEJ, MMEJ, ZFN, yeast

Introduction

DNA double-strand breaks (DSBs) are potentially toxic lesions that are repaired either by homologous recombination (HR), which uses an intact duplex as a template to restore the broken region, or by nonhomologous end joining (NHEJ), which directly ligates broken ends back together. In general, NHEJ is a more error-prone process, with out-of-register annealing between ends and/or end processing creating joints with small insertions or deletions. In addition, the rejoining of ends from different breaks can generate various types of genome rearrangements and has been implicated in recurrent oncogenic translocations. Although most DSBs are pathological and reflect either replication fork collapse, abortive topoisomerase reactions, or DNA damage, programmed DSBs breaks are essential in some biological processes. During meiosis, for example, the Spo11 protein creates DSBs that initiate the HR necessary for creating genetic diversity and for ensuring proper chromosome segregation (Keeney 2008). In mitosis, mating-type switching is initiated by the HO endonuclease in yeast (Haber 2012), and RAG proteins create DSBs that initiate the NHEJ-mediated joining of immunoglobulin gene segments in vertebrates (Jung *et al.* 2006).

DSB repair pathways are highly conserved, and the yeast *Saccharomyces cerevisiae* has served as a model for defining relevant proteins and molecular mechanisms. The broken ends of all types are bound by the Ku (Ku70–Ku80) and MRX (Mre11-Rad50-Xrs2) complexes; both are absolutely required for NHEJ in yeast (Daley *et al.* 2005b). Although not required for HR, MRX accelerates the initiation of 5′-end resection, which creates a 3′ tail that invades a homologous template and initiates HR [reviewed in Symington (2016) and Reginato and Cejka (2020)]. As part of the MRX complex, Mre11 nicks the 5′ terminated strand and subsequent 3′>5′ resection towards the break generates a free 3′ end. MRX activity is particularly important for eliminating end-attached proteins or terminal DNA damage and additionally removes Ku from ends to prevent NHEJ. In addition to its role in short-range resection, MRX facilitates the loading of long-range resection activities (Exo1 and Sgs1-Dna2) to promote efficient HR. HR requires a large suite of proteins to invade/copy the repair template as well as to resolve intermediates into final products [reviewed in Symington *et al.* (2014)]. In addition to Ku and MRX, NHEJ in yeast requires the dedicated Dnl4 DNA ligase (Teo and Jackson 1997) and the Pol4 DNA polymerase (Wilson and Lieber 1999).

Early NHEJ studies in yeast used transformation-based assays to assess the closure efficiency of linearized plasmids with defined end structures and to molecularly define the ligated products [reviewed in Daley *et al.* (2005b)]. An advantage of this type of system is that the end sequence can be manipulated in vitro to yield completely or partially complementary ends, or to generate completely incompatible ends (e.g. blunt ends or ends with different

Received: May 03, 2023. **Accepted:** June 16, 2023

polarity). With ends that have complementarity, the default is simple re-ligation. Following the annealing of ends with partial complementarity, gaps flanking the annealed region must be filled before ligation occurs. With 5′ overhangs, the filling of associated gaps is primed from a stably base-paired 3′ end. With 3′ overhangs, however, gap filling must occur from a 3′ end stabilized by at most a few base pairs and is more dependent on Pol4 (Daley *et al.* 2005a). In contrast to 3′ overhangs, the recessed 3′ ends of 5′ overhangs can directly be extended in the absence of end annealing. With overhangs that lack complementarity or are incompatible, joining usually involves processing-uncovered microhomologies that flank the broken ends.

Mitotic studies of DSB repair in a chromosomal context have relied on endonucleases that create a single, targeted DSB, and repair is monitored through selection of survivors or prototrophs. HO or I-*Sce*I, which generates breaks with 4-nt 3′ overhangs, have been used extensively to study error-prone DSB repair (e.g. Villarreal *et al.* 2012; Deng *et al.* 2014). Zinc finger nucleases (ZFNs), which create 4-nt 5′ overhangs, and Cas9, which mostly creates blunt ends, have only rarely been used (Liang *et al.* 2016; Lemos *et al.* 2018; Shaltz and Jinks-Robertson 2021). Because *S. cerevisiae* relies mainly on HR for the repair of genomic DSBs, NHEJ following endonuclease cleavage is studied either in the absence of a repair template or by disabling recombination. Precise rejoining of the ends by the NHEJ machinery regenerates the cleavage site, resulting in repetitive cycles of cleavage-ligation until a rare error-prone event renders the target sequence refractory to cleavage. Error-prone NHEJ typically involves minor addition or deletion of sequence from the broken ends and often reflects the annealing of small microhomologies within the overhangs, although microhomology is not a requirement. The overhang sequence dictates the spectrum of insertions/deletions, and this sequence cannot be varied when DSBs are initiated with I-*Sce*I or HO. In contrast, the use of a ZFN to create a DSB allows a manipulation of the 5′ overhang sequence (Liang *et al.* 2016; Shaltz and Jinks-Robertson 2021). Reflecting the different reactions that can occur at 5′ vs 3′ overhangs, the kinetics and fidelity of repair also differ (Liang *et al.* 2016).

In addition to the classical NHEJ pathway, yeast has an alternative end-joining pathway that is referred to as microhomology-mediated end-joining (MMEJ). MMEJ is characterized by its Ku independence and a requirement for 6–14 bp of microhomology [reviewed in Sfeir and Symington (2015)]. Finally, single-strand annealing (SSA) requires more extensive homology between direct repeats and is usually considered a variant of HR. In contrast to the canonical HR pathway, however, SSA is independent of the Rad51 strand-invasion protein (Ivanov *et al.* 1996), as is MMEJ (Lee and Lee 2007). The transition from MMEJ to SSA occurs when the microhomology reaches 15–20 bp and SSA, but not MMEJ, and has strong dependency on the Rad52 strand-annealing protein (Villarreal *et al.* 2012). It should be noted that higher eukaryotes lack a yeast-like MMEJ pathway and instead have an alternative end-joining pathway that is mediated by the Pol theta DNA polymerase (Sfeir and Symington 2015).

We previously described a system that used a galactose-induced ZFN to create a site-specific DSB in the yeast *LYS2* gene (Shaltz and Jinks-Robertson 2021). Insertion of an out-of-frame cleavage site allowed either the selection of NHEJ-mediated repair events that restored *LYS2* function or of repair events that simply allowed survival. Approximately, half of the latter were Ku-independent MMEJ events (Shaltz and Jinks-Robertson 2021). In the current study, this system was used to explore the genetic control of NHEJ- and MMEJ-mediated repair events.

Materials and methods

Haploid strains were used in all experiments and were derived from the W303 background (*leu2*-3,112 *his3*-11,15 *trp1*-1 *ura3 ade2*-1 *CAN1 RAD5*); each contained a galactose-inducible ZFN and a *lys2* frameshift allele containing the ZFN cleavage site. To measure the mean survival or Lys$^+$ revertant frequencies in growing cells continuously expressing the ZFN, mid-log cultures grown in raffinose-containing medium were plated on nonselective (YEP) or selective (lysine-deficient minimal) medium containing galactose. Saturated cultures were used to obtain a nongrowing (NG) cell population and G0 cells were isolated following incubation for 7 days. Spectra of error-prone repair events in Lys$^+$ revertants and in survivors were obtained by sequencing appropriate PCR products amplified from genomic DNA. Survival frequencies were adjusted so that they reflect the proportion of sequenced colonies that had lost the ZFN cleavage site. Details of experimental procedures and data analysis are provided in the Supplementary Material.

Results and discussion

A galactose-regulated, heterodimeric ZFN designed to cleave the Drosophila *rosy* locus (Beumer *et al.* 2006) was used to introduce a site-specific DSB in the *LYS2* gene (Shaltz and Jinks-Robertson 2021). Each ZFN subunit contained 3 zinc fingers and recognized a 9-bp target sequence flanking a spacer of sequence 5′-ACGAAT (Fig. 1a). Insertion of the 24-bp *rosy* target into *LYS2* created a −1 frameshift allele and net +1 mutations that restored the correct reading frame were selected by plating exponentially growing cultures on lysine-deficient medium containing galactose. Selection of surviving colonies on galactose-containing rich medium allowed a relatively unbiased assessment of events that eliminated the ZFN cleavage site. The genetic control of revertants, which reflected canonical NHEJ, and survivors, which reflected both NHEJ and MMEJ events, are described below.

Effects of core NHEJ components on ZFN-induced Lys$^+$ revertants

In a wild-type (WT) background, the frequency of Lys$^+$ prototrophs was 2.03×10^{-4} (Fig. 2a) and there were 3 major classes of NHEJ events, each of which accounted for approximately 30% of revertants (Fig. 2b; Shaltz and Jinks-Robertson 2021). The first class (69/226) had a CGAA insertion (+CGAA) resulting from the complete fill-in of each of the ZFN-generated 5′ overhangs (Fig. 1b). The second major class (59/226) contained a 2A > 3A expansion that is most easily explained by mis-annealing of the overhangs, followed by end trimming, gap filling, and ligation. In the third class of Lys$^+$ revertants (61/226), there was expansion to 2 thymines of a single thymine located immediately adjacent to the downstream ZFN-created overhang. We previously suggested that the 1T > 2T event reflects misincorporation of an adenine, followed by realignment/slippage that regenerates the 4-nt overhang for direct ligation. Among the remaining events was a recurrent 29-bp deletion with endpoints in a GCC repeat (4/226; Fig. 1c) as well as a variety of other minority events (33/226; see Supplementary Table 2).

We previously reported that the frequency of Lys$^+$ revertants decreased 4 orders of magnitude in a *yku70*Δ background (Shaltz and Jinks-Robertson 2021), and we observed a similar reduction in *dnl4*Δ and *mre11*Δ strains (Supplementary Table 1). Although Mre11 is required for NHEJ in yeast (Ma *et al.* 2003), loss of only its nuclease activity stimulates NHEJ-mediated repair of 3′ overhangs, presumably by slowing initiation of the processive 5′ end

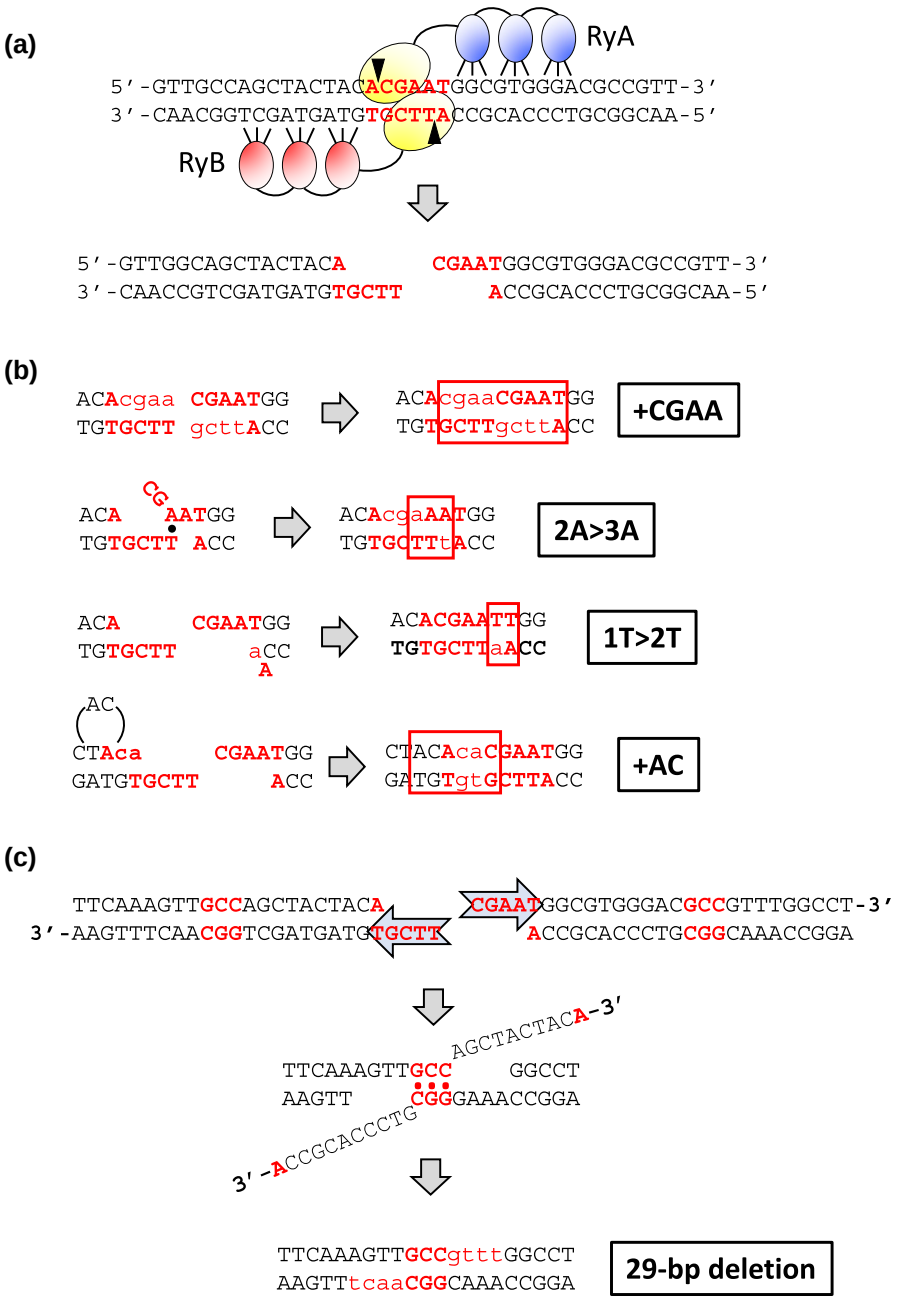

Fig. 1. ZFN cleavage of spacer ACGAAT and error-prone repair events. (A) The sequence of the 24-bp *rosy* sequence inserted into *LYS2* is shown, with the 3 bases recognized by each zinc finger indicated. The ovals represent the dimerized *Fok*I domains; the 6-bp spacer is in bold font, and triangles indicate the positions of enzyme-generated nicks that create 4-bp 5′ overhangs. (B) Sequences added during repair events are in lowercase. Only the first 3 classes (+CGAA, 2A > 3A, and 1T > 2T) generate Lys$^+$ revertants; the fourth class (+AC) was observed only among survivors. Complete filling of ends duplicates the region bounded by the ZFN nicks (+CGAA), while out-of-register pairing between an A and T in the overhangs generates the 2A > 3A mutation. Duplication of the T (1T > 2T) adjacent to the distal overhang can be generated by misincorporation-realignment, followed by ligation of the re-created 4-nt overhangs. The +AC event can be generated by a similar misincorporation-realignment mechanism during the initial filling of the proximal overhang. (C) Mechanism for the NHEJ-dependent 29-bp deletion that is frequent among Lys$^+$ revertants in the *pol4*Δ background. Resection of the 5′ ends allows pairing between GCC repeats (bold) that flank the DSB. Subsequent removal of 3′ tails and filling of flanking gaps (lowercase) completes the repair.

resection required for HR (Lee and Lee 2007; Deng *et al.* 2014). Introduction of the nuclease-dead *mre11-D56N* allele (Moreau *et al.* 1999) into the ZFN system similarly stimulated Lys$^+$ revertants 8-fold (Fig. 2a) but additionally was associated with an unanticipated change in the spectrum of NHEJ events (Fig. 2b; $P < 0.0001$). Thus, in addition to a general repressive effect on NHEJ, Mre11 nuclease activity altered molecular outcomes.

In contrast to the complete absence of Lys$^+$ prototrophs in *yku70*Δ, *dnl4*Δ, and *mre11*Δ backgrounds, there was only a 10-fold reduction in Lys$^+$ frequency when *POL4* was deleted (Fig. 2a), which is consistent with most, but not all, repair of HO-generated 3′ overhangs requiring Pol4 (Lee and Lee 2007; Tseng *et al.* 2008). A similar Pol4 dependence of NHEJ was observed using plasmids with defined 3′ overhangs but, in contrast to the

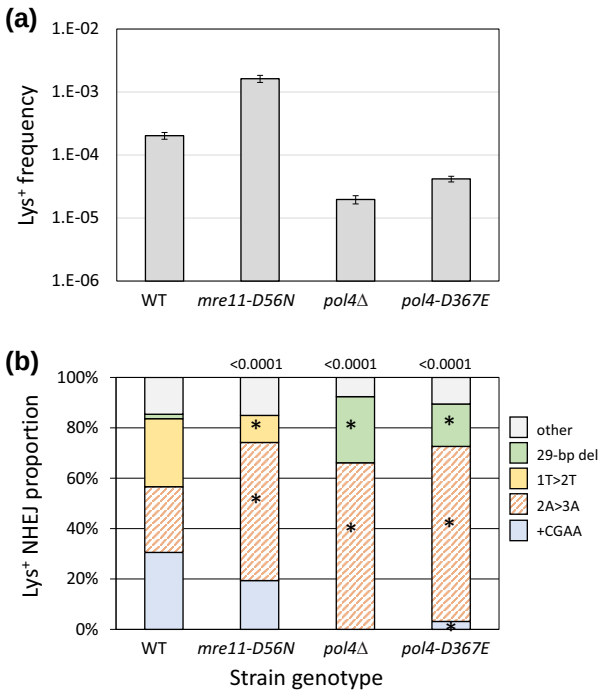

Fig. 2. Frequencies and distributions of Lys+ revertants in strains with altered core NHEJ proteins. a) Mean frequencies of Lys+ colonies; error bars are 95% confidence intervals for the mean. b) Distributions of the 5 major NHEJ types among revertants. Overall distributions were compared to WT using a global 2 × 5 contingency chi-square test (*P*-values are above each spectrum) and if $P < 0.05$, then individual mutation types were compared using the Bonferroni correction to determine significance ($P < 0.05/5$); asterisks indicate a significant proportional class increase/decrease.

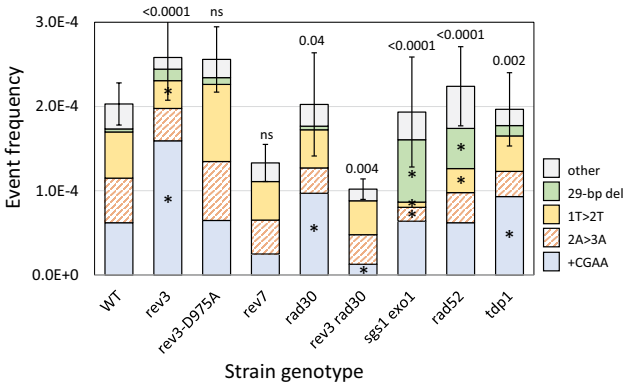

Fig. 3. Altered frequencies and distributions of Lys+ revertants in mutant backgrounds. Mean frequencies of Lys+ colonies are shown; error bars are 95% confidence intervals for the means. The overall distribution of the 5 major NHEJ types in each mutant background was compared to WT using a 2 × 5 contingency chi-square test (ns, not significant). If the global *P*-value (above each spectrum) was less than 0.05, individual mutation classes were compared using the Bonferroni correction to determine significance ($P < 0.05/5$); asterisks indicate a significant proportional increase/decrease.

ZFN ends generated here in a chromosomal context, there was little or no Pol4 dependence with 5′ overhangs (Daley *et al.* 2005a). Of the 3 major classes of Lys+ events observed following ZFN cleavage, only the 2A > 3A event (121/183 revertants analyzed) persisted; there were no +CGAA or 1T > 2T events detected (Fig. 2b). A feature of the 2A > 3A event that distinguishes it from the 1T > 2T and +CGAA events is that it can occur through the annealing of 5′ tails, suggesting that Pol4 may be somewhat less important for gap-filling than for end-filling reactions. Of particular note, the 29-bp deletion event that was rare in WT (~2%; 4/226) accounted for 26% (48/183) of ZFN-initiated events in the *pol4*Δ background. When converted to frequencies, Pol4 loss reduced the 2A > 3A frequency 5-fold but had no effect on the 29-bp deletion. Finally, the relative importance of Pol4 presence vs its polymerase activity during NHEJ was examined using the *pol4-D367E* allele, which encodes a catalytically inactive protein (Wilson and Lieber 1999). While the Lys+ spectrum in the *pol4-D367E* background was identical to that in the *pol4*Δ mutant, the frequency of Lys+ revertants was 2-fold higher than in the *pol4*Δ strain. This suggests a minor structural role for Pol4 not previously detected (Wilson and Lieber 1999), which could reflect the stimulation of Dnl4-mediated ligation by Pol4 reported in vitro (Tseng and Tomkinson 2002).

Effects of additional proteins on NHEJ-mediated repair of a ZFN-initiated break

The persistence of Lys+ colonies in the *pol4*Δ mutant indicates involvement of other DNA polymerases during repair of 5′ overhangs. The Pol ϵ replicative polymerase has been implicated, for example, in tail removal following the annealing of 3′ overhangs (Tseng *et al.* 2008). In the current study, we focused on roles of the translesion synthesis (TLS) polymerases Pol ζ and Pol η; *REV3* encodes the catalytic subunit of Pol ζ while the single subunit Pol η protein is encoded by *RAD30*. As observed following cleavage that generates 3′ overhangs (Lee and Lee 2007), there was no significant change in the Lys+ frequency in the *rev3*Δ or *rad30*Δ single mutant. There was, however, a significant change in the proportional distribution of NHEJ events in each mutant (Fig. 3). In the *rev3*Δ spectrum the proportion of +CGAA events increased 2-fold and accounted for 62% of events (58/94); the proportional decrease in 1T > 2T events was significant (12/94) while that of 2A > 3A events was not (14/94).

Rev3 associates with chromatin near an HO-generated DSB (Hirano and Sugimoto 2006), and we used the *rev3-D975A* allele (Johnson *et al.* 2012) to determine whether the alteration in the NHEJ outcomes in the *rev3*Δ background reflects the presence of the protein or requires its catalytic activity. Both the frequency and spectrum of Lys+ colonies in the *rev3-D975A* catalytic mutant (Johnson *et al.* 2012) were indistinguishable from those of the WT parent, indicating that it is the presence of Rev3 that affects NHEJ outcomes. Rev7 interacts with Rev3 as part of the Pol ζ holoenzyme, and we also examined its role in NHEJ. The effect of *REV7* deletion was distinct from that of *REV3* loss. Whereas the spectrum but not the frequency of Lys+ revertants was altered in the *rev3*Δ background, there was a slight reduction in frequency but the spectrum was unchanged in the *rev7*Δ mutant. The human equivalent of Rev7 (REV7, also known as MAD2L2) restrains end resection to limit HR and promote NHEJ (Xu *et al.* 2015). Although a similar role for the yeast Rev7 has not been reported, the reduced NHEJ frequency in the *rev7*Δ background is suggestive of more robust resection in its absence.

In the *rad30*Δ background, the frequency of Lys+ revertants was not altered but there again was a significant change in the spectrum of NHEJ events ($P = 0.019$). As in the *rev3*Δ background, the proportion of +CGAA events was elevated (45/94; $P = 0.0047$); the proportion of the 2A > 3A or 1T > 2T events was not significantly altered ($P > 0.0125$). Whereas individual deletion of *REV3* or *RAD30* affected the spectrum but not the frequency of Lys+ revertants, simultaneous deletion of both was associated with a 2-fold

reduction in Lys+ frequency as well as a change in the NHEJ spectrum ($P = 0.0027$). Instead of the proportional *increase* in +CGAA events observed in the single mutants, there was a specific *decrease* of this specific class in the *rev3*Δ *rad30*Δ double mutant. While the explanation for this is not obvious, especially given the *POL4* dependence of the +CGAA event, it underscores the complexity of interactions that take place during the error-prone repair of broken ends.

NHEJ-mediated repair in *rad52*Δ and *sgs1*Δ *exo1*Δ backgrounds was examined while measuring potential effects on MMEJ events in surviving colonies. The Rad52 protein is essential for HR and previous studies have reported either no (Frank-Vaillant and Marcand 2002; Villarreal *et al.* 2012) or very small changes (Deng *et al.* 2014) in NHEJ frequency in a *rad52*Δ background. Sgs1 and Exo1 are redundantly required for the processive resection of 5′ ends (Mimitou and Symington 2008) and their loss has no effect on NHEJ (Villarreal *et al.* 2012; Deng *et al.* 2014). While we similarly detected no significant change in the Lys+ frequency in either a *rad52*Δ or *sgs1*Δ *exo1*Δ background, the distribution of revertant types was altered in each (Fig. 3). Particularly striking was the elevation in "other" NHEJ events: from 16% (37/226) in WT to 44% (41/94) in the *rad52*Δ and to 55% (52/94) in the *sgs1*Δ *exo1*Δ strain. In both backgrounds, this change reflected a significant increase in the Pol4-independent 29-bp deletion. A distinguishing feature of this specific NHEJ event is that it presumably requires at least some resection to expose complementary repeats, although it is limited by the processive resection of Sgs1/Exo1. If processive resection occurs normally, the data suggest that the 29-bp deletion may remain an option only if recombination cannot be initiated (*rad52*Δ background).

Yeast tyrosyl DNA phosphodiesterase (Tdp1) resolves the 5′- and 3′-phosphotyrosyl linkages associated with stabilized topoisomerases (Pouliot *et al.* 1999; Nitiss *et al.* 2006) and has a 3′ nucleosidase activity that generates 3′-phosphate termini (Interthal *et al.* 2005). Consistent with the latter activity, deletion of *TDP1* was associated with an increase in the complete fill-in of 5′ overhangs in a plasmid-based NHEJ assay (Bahmed *et al.* 2010). A similar effect was not observed, however, when repair of a ZFN-generated chromosomal break was examined by deep sequencing (Liang *et al.* 2016). In our system, *TDP1* deletion had no effect on the frequency of Lys+ revertants but did alter the spectrum of events ($P = 0.013$). Among the 3 major classes of events, there was a significant change only in the proportion of +CGAA events (from 69/226 in WT to 53/112 in *tdp1*Δ; $P = 0.0055$). This is consistent with a subtle effect on Tdp1 on the ability to fill 5′ overhangs.

Genetic control of the Pol4-independent 29-bp deletion

The model for the 29-bp deletion, which accounted for 26% of revertants in the *pol4*Δ background, requires 5′>3′ resection to expose GCC repeats that flank the ZFN cleavage site, annealing between complementary strands of GCC repeats, and cleavage of single-strand 3′ tails to allow filling of flanking gaps (Fig. 1c). We first examined whether TLS polymerases are relevant to the Pol4-independent filling of the small gaps flanking the annealed segment. *REV3*, *RAD30*, or both were deleted from the *pol4*Δ background and there were changes in the frequency and/or spectra of Lys+ revertants in each relative to the *pol4*Δ single mutant (Fig. 4). The Lys+ frequency increased 2.0- and 3.7-fold, respectively, in the *pol4*Δ *rad30*Δ and *pol4*Δ *rev3*Δ backgrounds but was not significantly altered in the *pol4*Δ *rev3*Δ *rad30*Δ triple mutant. The proportion of the 29-bp deletion was reduced in the *pol4*Δ *rev3*Δ and *pol4*Δ *rev3*Δ *rad30*Δ backgrounds but was unaffected in the *pol4*Δ

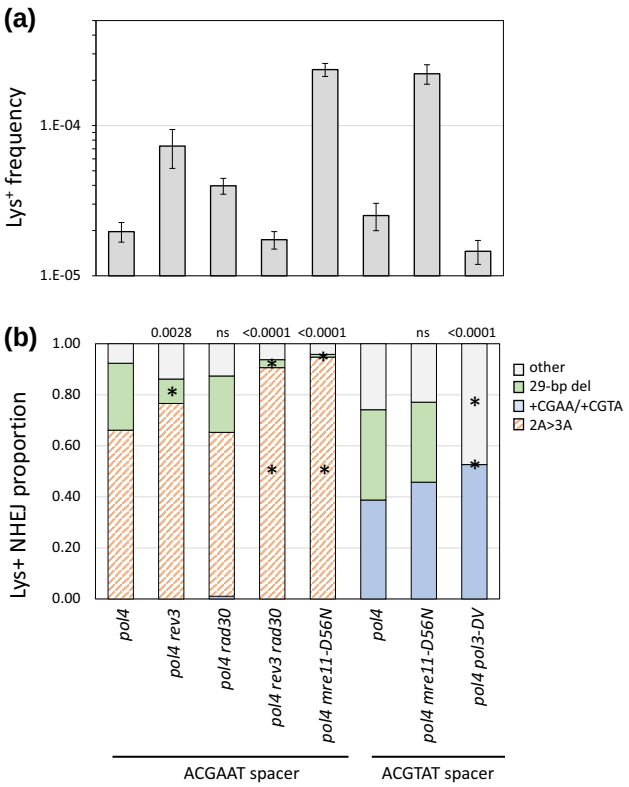

Fig. 4. Genetic control of the Pol4-independent, 29-bp deletion. a) Mean frequencies of Lys+ colonies; error bars are 95% confidence intervals for the means. b) The overall distribution of the 3 major NHEJ types in each mutant background. With the ACGAAT spacer only the 2A > 3A, the 29-bp deletion, and random "other" events were observed; there were no 1T > 2T or +CGAA events. Changing the ACGAAT spacer to ACGTAT eliminated the 2A > 3A event, which was replaced by +CGTA. Each distribution was compared to the corresponding WT using a 2 × 3 contingency chi-square test (ns, not significant). If the global *P*-value (above each spectrum) was less than 0.05, individual mutation classes were compared using the Bonferroni correction to determine significance ($P < 0.05/3$); asterisks indicate a significant proportional increase/decrease.

*rad30*Δ mutant. The frequencies of the 29-bp deletion were estimated by multiplying Lys+ frequencies and corresponding proportions of the 29-bp deletion. The 29-bp deletion frequency was unaffected by the deletion of *REV3* or *RAD30* individually in the *pol4*Δ background but was reduced 10-fold in the *pol4*Δ *rev3*Δ *rad30*Δ triple mutant. These data demonstrate that Pol ζ and Pol η have redundant roles during the Pol4-independent gap filling required to generate the 29-bp deletion.

Although sporadic deletions involving other short repeats were observed among revertants in all genetic backgrounds (Supplementary Table 2), the GCC repeats at the endpoint of the 29-bp deletion were notable because they are close to and symmetrically flank the ZFN cleavage site. Furthermore, the frequency of the 29-bp deletion was elevated when the long-range resection pathways were eliminated (*exo1*Δ *sgs1*Δ double mutant; Fig. 3). Given the repressive effect of resection on this event and the symmetry/proximity of the GCC repeats to the ZFN cleavage site, we considered the possibility that Mre11 nuclease activity might be required to expose the repeats within short 3′ overhangs. Mre11 nicks the 5′ strand 30–35 nt from a Ku-bound end and expansion of the nick into a gap by its 3′>5′ exonuclease activity degrades the 5′ end to displace Ku and create a short 3′ tail [reviewed in Reginato and Cejka (2020)]. To examine the relevance of Mre11

nuclease activity to the NHEJ-dependent 29-bp deletion, the nuclease-dead *mre11-D56N* allele (Llorente and Symington 2004) was introduced into the *pol4*Δ background. The Lys$^+$ frequency increased 12-fold in the double mutant relative to the *pol4*Δ single mutant, and this was accompanied by a change in the distribution of revertant types (Fig. 4). Almost all revertants had the 2A > 3A event (91/96; $P < 0.0001$), and only a single 29-bp deletion was observed. The *mre11-D56N* allele thus had a strong stimulatory effect on the frequency 2A > 3A event, but its effect on the frequency of the 29-bp deletion was unclear.

To preclude the occurrence of the 2A > 3A event and allow more specific focus on the 29-bp deletion in the *pol4*Δ background, we changed the spacer sequence of the ZFN cleavage site from ACGAAT to ACGTAT. With the new ACGTAT spacer in the *POL4* background, there were similar numbers of +CGTA and 1T > 2T events (43/116 and 63/116, respectively), as there were with the original spacer, and the 29-bp deletion remained rare (2/116). Given the absence of +4 and 1T > 2T events with the original ACGAAT spacer in the *pol4*Δ background, we assumed that the 29-bp deletion would be present in almost all Lys$^+$ colonies derived using the new ACGTAT spacer. In the *pol4*Δ background with the new spacer, however, half of revertants contained the +CGTA event (54/37) and 30% had the 29-bp deletion (37/118); there still were no 1T > 2T events. In the absence of Pol4, the data suggest that the end annealing that generates the 2A > 3A event may precede complete filling and obscure its occurrence.

Elimination of Mre11 nuclease activity in a *POL4* background with the new spacer increased the frequency of Lys$^+$ revertants 14-fold and altered the proportions of +CGTA and 1T > 2T events (Supplementary Tables 1 and 2). This mirrors the differential effects of the *mre11-D56N* allele on the NHEJ spectrum observed with the original ACGAAT spacer. Introduction of the *mre11-D56N* allele into the *pol4*Δ background resulted in a 9-fold increase in Lys$^+$ frequency relative to the *pol4*Δ single mutant, which was similar to the increase observed with the original spacer. In contrast to the large proportional decrease in the 29-bp deletion in the *pol4*Δ *mre11-D56N* background with original spacer, however, there was no reduction with the new spacer. This demonstrates that Mre11 nuclease activity is not required to expose the GCC repeats at the endpoints of the 29-bp deletion.

In the model depicted in Fig. 1c end resection allows annealing between complementary strands of the GCC repeat, thereby creating 3′ tails that must be removed prior to gap filling and ligation. The Rad1–Rad10 nuclease is required for the removal of long 3′ tails during SSA, but tails <30 nt are efficiently removed by the exonuclease activity of Pol δ (Paques and Haber 1997). In the *pol4*Δ strain containing the new spacer sequence, elimination of the exonuclease activity of Pol δ (*pol3-DV* allele; Jin *et al.* 2001) reduced the Lys$^+$ frequency 2.5-fold and this reflected the complete absence of the 29-bp deletion among revertants (0/95 revertants; $P < 0.0001$; Fig. 4). These data demonstrate that the exonuclease activity of Pol δ is required during the creation of the 29-bp deletion.

The data presented above present a conundrum with respect to the genetic control of the NHEJ-dependent 29-bp deletion. It was antagonized by processive nuclease activity (*sgs1*Δ *exo1*Δ background) and yet did not appear to depend on the nuclease activity of Mre11 (*pol4*Δ *mre11-D56N* background). How then are the complementary strands of the GCC direct repeats exposed? One possibility is that the DNA melting activity of the MRX complex is responsible. This requires the ATPase activity of Rad50 (Cannon *et al.* 2013), which also is required for NHEJ in yeast (Zhang and Paull 2005). The strong dependence of the 29-bp deletion on the exonuclease activity of Pol δ (*pol4*Δ *pol3-DV* mutant) suggests an alternative possibility in which it is the degradation of the recessed 3′ ends by Pol δ that exposes the GCC repeats. Regardless of how the complementary strands of the GCC repeats are exposed, the Ku dependence of the 29-bp deletion suggests either that Ku remains associated with the ends or that Ku re-engages the ends after displacement. Ku interacts with duplexes with 30-nt tails almost as well as with fully duplex DNA in vitro (Falzon *et al.* 1993); longer, 60-nt tails are not efficiently bound by Ku (Foster *et al.* 2011).

Survivors of continuous ZFN expression

Selection for colonies on rich medium containing galactose provides an unbiased analysis of end-joining events that confer resistance to continuous ZFN expression. As reported previously, only half of survivors (83/155) in the WT background lost the enzyme cleavage site (Shaltz and Jinks-Robertson 2021), and these were of 2 major types: a Ku-dependent +AC event that expanded 2 copies an AC dinucleotide spanning the 6-bp ZFN spacer (36/83) and Ku-independent large deletions that removed the cleavage site (47/83). The +AC event was not detectable in the reversion assay, which selects net +1 events, and was hypothesized to arise by misincorporation-slippage during proximal end filling (Fig. 1b). The rarity of net +1 events in the survivor assay indicates that they are minor events relative to +AC. The large deletions were either 1.2 kb (36/47) or 11.7 kb (11/47) in size (Fig. 5a), and because the deletion junctions were in 13- or 14-bp direct repeats, respectively, we concluded that these were MMEJ events. In the current analyses, the frequencies and profiles of survivors were examined in the genetic backgrounds described above for Lys$^+$ revertants. Only those mutants that were different from the WT strain in terms of the frequency and/or spectrum of site-loss survivors are discussed (see Supplementary Tables 1 and 3 for all data).

Because NHEJ and MMEJ proportions are similar among survivors, the complete loss of either pathway would be expected to reduce the survival frequency only 2-fold. Indeed, as reported previously in the *yku70*Δ background (Shaltz and Jinks-Robertson 2021), the survival frequency was reduced 2-fold in the NHEJ-deficient *pol4*Δ (Fig. 5b and c) and *dnl4*Δ (Supplementary Tables 1 and 3) backgrounds and only large deletions were detected. Although NHEJ events were also absent in an *mre11*Δ strain, there was 5.9-fold reduction in overall survival frequency rather than the expected 2-fold (Fig. 5b). The *mre11*Δ strain grew poorly relative to the other NHEJ-defective strains, and this likely accounts for the reduced survival (see below). Another difference between the *mre11*Δ and other NHEJ-defective strains was an altered distribution of the 11.7 and 1.2 kb deletions relative to the WT strain. Among survivors in the WT strain, the 11.7 kb deletion comprised 25% (11/47) of MMEJ events and this proportion was not significantly altered in *yku70*Δ, *pol4*Δ, or *dnl4*Δ background (Supplementary Table 3). In the *mre11*Δ strain, however, only one of 47 MMEJ events contained the 11.7 kb deletion ($P = 0.0018$). A distinguishing feature of the 2 MMEJ events is that one endpoint of the 1.2 kb deletion is next to the ZFN cleavage site, while each endpoint of the 12 kb deletion is 5–6 kb from the cleavage site. The reduction in the 11.7 kb deletion, which uniquely requires extensive resection from both ends, is consistent with the role of the MRX complex in coordinating end resection (Westmoreland and Resnick 2013). In contrast to the *mre11*Δ mutant, no reduction in the 11.7 kb MMEJ event was associated with the loss of Mre11 nuclease activity (*mre11-D56N* strain).

As in the *mre11*Δ strain, survivor frequencies were low in *rad52*Δ single and *sgs1*Δ *exo1*Δ double-mutant backgrounds, with reductions of 6.7- and 16.7-fold, respectively, relative to WT. Impaired

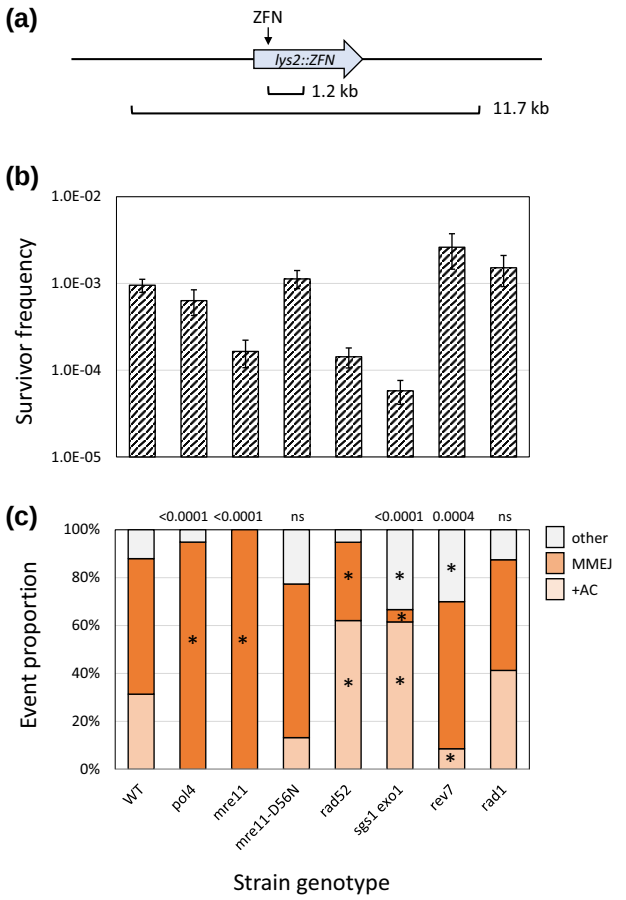

Fig. 5. Genetic control of the survivor frequency and spectrum. a) The 2 types of recurrent large deletions detected among surviving colonies. The 1.2 kb deletion has endpoints in 13-bp direct repeats (CCAAGCTACTACA), one of which overlaps the DNA binding site of the RyB subunit of the ZFN. The 11.7 kb deletion has endpoints in 14-bp direct repeats (TGGAAAAAAAAAAA) and removes the *LYS2*-flanking genes *TKL2* and *RAD16* (not shown). b) Mean frequencies of surviving colonies that lost the ZFN cleavage site; error bars are 95% confidence intervals for the means. c) The distributions of the 3 major survivor types are shown. Each mutant distribution was compared to the WT using a 2×3 contingency chi-square test (ns, not significant). If the global *P*-value (above each spectrum) was less than 0.05, individual mutation classes were compared using the Bonferroni correction to determine significance ($P < 0.05/3$); asterisks indicate a significant proportional increase/decrease.

growth was a common feature of these 3 mutant backgrounds, and we suggest that this may be responsible for the large decrease in survivor frequency. We favor this interpretation because, in contrast to the survivor assay, the NHEJ frequency as measured by Lys$^+$ reversion was not affected in either the *rad52*Δ or *sgs1*Δ *exo1*Δ background (Fig. 3). It is possible that repetitive cleavage by a ZFN impairs viability more when cells can continue to divide (nonselective rich medium) than when cells are plated under conditions where error-prone repair must restore prototrophy before cells can begin dividing.

In addition to reduced survival, the spectrum of events among survivors was altered in the *rad52*Δ and *sgs1*Δ *exo1*Δ backgrounds relative to WT ($P = 0.0013$ and $P < 0.0001$, respectively). There was a reduction in the proportion of large deletions in the *rad52*Δ mutant, (from 47/83 to 19/58; $P = 0.009$), suggestive of a partial requirement of Rad52 for the MMEJ-mediated large deletions. In an earlier study that systematically examined the effect of repeat size on MMEJ (Villarreal *et al.* 2012), Rad52 promoted end joining for repeats 15 bp or larger, suggesting a variation of SSA as the mechanism, and strongly inhibited end-joining between repeats 12 bp or smaller. The sizes of the repeats at the MMEJ endpoints in the current study (13–14 bp) are in the transition zone for Rad52 dependence. In the *sgs1*Δ *exo1*Δ double mutant, the proportion of large deletions was reduced 10-fold: from 47/83 in WT to only 2/39. This reduction likely reflects the extensive resection required to expose the junction repeats of large deletions and is consistent with results obtained with similar large deletions (Villarreal *et al.* 2012). This is in contrast to the suppressive effect of Sgs1/Exo1 resection (as well as Mre11 presence) with respect to Ku-independent deletions between 12-bp repeats very close to I-*Sce*I-generated ends (Deng *et al.* 2014). The resection-related suppression is similar to that described above for the Pol4-independent 29-bp deletion, although the 29-bp deletion is Ku- and Mre11-dependent (see above).

Because the nuclease activity of Mre11 inhibits NHEJ, an elevation in the NHEJ-dependent +AC event was expected in an *mre11-D56N* background. There, however, was neither a change in survivor frequency nor spectrum relative to WT. This result provides further support for an influence of Mre11 nuclease activity on specific NHEJ outcomes, as inferred from the variable effect of the *mre11-D56N* allele on Lys$^+$ revertant types in the WT and *pol4*Δ backgrounds. Finally, there was 2.7-fold increase in survivor frequency in a *rev7*Δ background that specifically reflected an increase in MMEJ; no effect on frequency or spectra was observed upon loss of *REV3* (Supplementary Table 1). These data more strongly support a potentially suppressive role of Rev7 on processive resection in yeast, as inferred previously from the slightly increased frequency of Lys$^+$ revertants.

The Rad1–Rad10 endonuclease is required to remove 3′ tails during SSA (Ivanov and Haber 1995) and a similar importance for Rad1 in MMEJ was inferred through analysis of HO-initiated 2-kb deletions between 18-bp direct repeats (Villarreal *et al.* 2012). The strong Rad52 dependence for deletions between 18-bp, however, suggests that the events were a variation of SSA. We thus re-examined the requirement for Rad1 for the large, NHEJ-independent deletions in our system. With the smaller (13- and 14-bp) repeats, there was no significant change in either the frequency or the distribution of survivor types in a *rad1*Δ background (Fig. 5; see Supplementary Tables 1–3 for similar *rad10*Δ data). To potentially identify the relevant structure-specific nuclease that removes 3′ tails during MMEJ, we examined survival in *mus81*Δ single and *rad1*Δ *mus81*Δ double mutants, as well as in an *slx4*Δ background. Mus81 can process 3′ flaps (Schwartz and Heyer 2011) while Slx4 is a scaffold for multiple structure-specific endonucleases (Cussiol *et al.* 2017). There was no proportional decrease in large deletions in any of these additional mutant backgrounds (Supplementary Table 3). Either a different nuclease is relevant, or there is functional redundancy between the nucleases examined. Just as there is a size-related transition in Rad52 dependence for microhomology-mediated deletions (Villarreal *et al.* 2012), there may be a similar transition in terms of a requirement for Rad1–Rad10 in 3′-tail removal. One interesting possibility is that Rad52-driven annealing dictates whether subsequent tail removal is dependent on Rad1–Rad10.

The physiological state of cells affects repair of ZFN-induced DSBs

NHEJ-mediated ligation of a linearized plasmid is more efficient when non-growing (NG) cells are transformed than when growing cells are transformed (Karathanasis and Wilson 2002). To examine the effects of growth state on error-prone repair of a

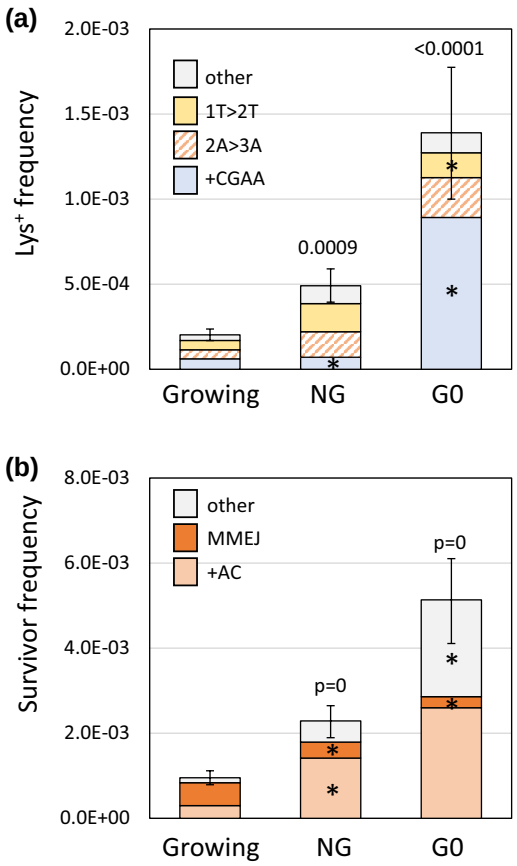

Fig. 6. Alterations in error-prone DSB repair in NG and G0 cells. a) Mean Lys$^+$ frequencies and revertant-type distributions in growing, NG and G0 cells. b) Mean survivor frequencies and event-type distributions in growing, NG and G0 cells. Error bars are 95% confidence intervals for mean frequencies. Event-type distributions were compared to growing cells using a 2×4 or 2×3 contingency chi-square test for revertants or survivors, respectively; ns, not significant. If the global *P*-value was <0.05 (above each spectrum), then individual mutation types were compared using the Bonferroni correction to determine significance; asterisks indicate a significant proportional increase/decrease.

chromosomal DSB, either NG or isolated G0 cells were plated in the presence of galactose. The Lys$^+$ frequency in NG cells was 2.4-fold higher than in growing cells, and there were proportionally fewer +CGAA events among revertants (Fig. 6a). When the event types were converted to frequencies, however, the +CGAA frequency was unaltered while the frequencies of 2A > 3A, 1T > 2T, and other NHEJ events were each elevated about 3-fold. There was a further stimulation of the Lys$^+$ frequency when G0 cells were plated: 6.8- and 2.8-fold relative to growing and NG cells, respectively. Interestingly, there was a very large proportional increase in the +CGAA class of events in G0 cells that corresponded to a 10-fold increase in its frequency relative to growing/NG cells; the frequencies of the other classes changed little relative to NG cells.

In terms of surviving colonies that had lost the ZFN cleavage site, the overall frequency also was elevated relative to growing cells: 2.4-fold in NG cells and 5.4-fold in G0 cells (Fig. 6b). The spectrum of survivors was also altered. As expected of events that require extensive resection, the proportion of large deletions was greatly reduced: from 0.56 (47/83) in growing cells to 0.16 (15/92) and 0.05 (4/79) when NG and G0 cells, respectively, were plated. Given the large increase in survival, however, the large-deletion frequency was reduced only about 2-fold in NG and G0 cells. In terms of frequency, the +AC event was elevated 4.7-fold in NG cells and 8.7-fold in G0 cells; the frequency of "other" events was similarly elevated. The data demonstrate that NHEJ-mediated repair of a ZFN-generated DSB is more efficient in NG/G0 cells than in growing cells, and that physiological state additionally affects how the resulting ends are modified during error-prone repair.

Conclusions

- Following ZFN cleavage, half of error-prone repair events among survivors reflected small insertions/deletions at the cleavage site (NHEJ), and half were large deletions (MMEJ).
- In contrast to the complete dependence of NHEJ on Ku, Mre11, and Dnl4, loss of Pol4 reduced NHEJ only 10-fold. Although most NHEJ events were dependent on Pol4, a recurrent 29-bp deletion was Pol4-independent. This deletion was suppressed by processive 5′ end resection and required the 3′ >5′ exonuclease activity of the replicative DNA polymerase δ.
- Mre11 nuclease activity suppressed NHEJ and additionally affected the spectrum of events but had no effect on MMEJ.
- Pol ζ and Pol η altered NHEJ outcomes in both the presence and the absence of Pol4.
- Absence of the Rev3 or Rev7 component of Pol ζ had different effects on DSB repair. Of particular note, the suppressive effect of Rev7 on MMEJ is consistent with a modulation of resection.
- Long single-strand tails created by resection must be removed to complete MMEJ, but neither Rad1, Mus81, nor Sxl4 was required for this step.
- NHEJ was increased and MMEJ was decreased when ZFN cleavage occurred in nondividing cells.

Data availability

Strains and plasmids are available upon request. The authors affirm that all data necessary for confirming the conclusions of the article are present within the article, figures, and tables.

Supplemental material available at GENETICS online

Funding

This work was supported by National Institutes of Health grant R35GM118077 to SJR.

Conflicts of interest

The author(s) declare no conflict of interest.

Literature cited

Bahmed K, Nitiss KC, Nitiss JL. Yeast Tdp1 regulates the fidelity of nonhomologous end joining. Proc Natl Acad Sci USA. 2010; 107(9):4057–4062. doi:10.1073/pnas.0909917107.

Beumer K, Bhattacharyya G, Bibikova M, Trautman JK, Carroll D. Efficient gene targeting in Drosophila with zinc-finger nucleases. Genetics. 2006;172(4):2391–2403. doi:10.1534/genetics.105.052829.

Cannon B, Kuhnlein J, Yang SH, Cheng A, Schindler D, Stark JM, Russell R, Paull TT. Visualization of local DNA unwinding by Mre11/Rad50/Nbs1 using single-molecule FRET. Proc Natl Acad Sci USA. 2013;110(47):18868–18873. doi:10.1073/pnas.1309816110.

Cussiol JR, Dibitetto D, Pellicioli A, Smolka MB. Slx4 scaffolding in homologous recombination and checkpoint control: lessons from yeast. Chromosoma. 2017;126(1):45–58. doi:10.1007/s00412-016-0600-y.

Daley JM, Laan RL, Suresh A, Wilson TE. DNA joint dependence of pol X family polymerase action in nonhomologous end joining. J Biol Chem. 2005a;280(32):29030–29037. doi:10.1074/jbc.M505277200.

Daley JM, Palmbos PL, Wu D, Wilson TE. Nonhomologous end joining in yeast. Annu Rev Genet. 2005b;39(1):431–451. doi:10.1146/annurev.genet.39.073003.113340.

Deng SK, Gibb B, de Almeida MJ, Greene EC, Symington LS. RPA antagonizes microhomology-mediated repair of DNA double-strand breaks. Nat Struct Mol Biol. 2014;21(4):405–412. doi:10.1038/nsmb.2786.

Falzon M, Fewell JW, Kuff EL. EBP-80, a transcription factor closely resembling the human autoantigen Ku, recognizes single- to double-strand transitions in DNA. J Biol Chem. 1993;268(14):10546–10552. doi:10.1016/S0021-9258(18)82233-5.

Foster SS, Balestrini A, Petrini JH. Functional interplay of the Mre11 nuclease and Ku in the response to replication-associated DNA damage. Mol Cell Biol. 2011;31(21):4379–4389. doi:10.1128/MCB.05854-11.

Frank-Vaillant M, Marcand S. Transient stability of DNA ends allows nonhomologous end joining to precede homologous recombination. Mol Cell. 2002;10(5):1189–1199. doi:10.1016/S1097-2765(02)00705-0.

Haber JE. Mating-type genes and *MAT* switching in *Saccharomyces cerevisiae*. Genetics. 2012;191(1):33–64. doi:10.1534/genetics.111.134577.

Hirano Y, Sugimoto K. ATR homolog Mec1 controls association of DNA polymerase ζ-Rev1 complex with regions near a double-strand break. Curr Biol. 2006;16(6):586–590. doi:10.1016/j.cub.2006.01.063.

Interthal H, Chen HJ, Champoux JJ. Human Tdp1 cleaves a broad spectrum of substrates, including phosphoamide linkages. J Biol Chem. 2005;280(43):36518–36528. doi:10.1074/jbc.M508898200.

Ivanov EL, Haber JE. *RAD1* and *RAD10*, but not other excision repair genes, are required for double-strand break-induced recombination in *Saccharomyces cerevisiae*. Mol Cell Biol. 1995;15(4):2245–2251. doi:10.1128/MCB.15.4.2245.

Ivanov EL, Sugawara N, Fishman-Lobell J, Haber JE. Genetic requirements for the single-strand annealing pathway of double-strand break repair in *Saccharomyces cerevisiae*. Genetics. 1996;142(3):693–704. doi:10.1093/genetics/142.3.693.

Jin YH, Obert R, Burgers PM, Kunkel TA, Resnick MA, Gordenin DA. The 3′–>5′ exonuclease of DNA polymerase δ can substitute for the 5′ flap endonuclease Rad27/Fen1 in processing Okazaki fragments and preventing genome instability. Proc Natl Acad Sci USA. 2001;98(9):5122–5127. doi:10.1073/pnas.091095198.

Johnson RE, Prakash L, Prakash S. Pol31 and Pol32 subunits of yeast DNA polymerase δ are also essential subunits of DNA polymerase ζ. Proc Natl Acad Sci USA. 2012;109(31):12455–12460. doi:10.1073/pnas.1206052109.

Jung D, Giallourakis C, Mostoslavsky R, Alt FW. Mechanism and control of V(D)J recombination at the immunoglobulin heavy chain locus. Annu Rev Immunol. 2006;24(1):541–570. doi:10.1146/annurev.immunol.23.021704.115830.

Karathanasis E, Wilson TE. Enhancement of *Saccharomyces cerevisiae* end-joining efficiency by cell growth stage but not by impairment of recombination. Genetics. 2002;161(3):1015–1027. doi:10.1093/genetics/161.3.1015.

Keeney S. Spo11 and the formation of DNA double-strand breaks in meiosis. In: Egel R, Lankenau DH, editors. Genome Dynamics and Stability. Vol. 2. Berlin, Heidelberg: Springer; 2008. p. 81–123.

Lee K, Lee SE. *Saccharomyces cerevisiae* Sae2- and Tel1-dependent single-strand DNA formation at DNA break promotes microhomology-mediated end joining. Genetics. 2007;176(4):2003–2014. doi:10.1534/genetics.107.076539.

Lemos BR, Kaplan AC, Bae JE, Ferrazzoli AE, Kuo J, Anand RP, Waterman DP, Haber JE. CRISPR/Cas9 cleavages in budding yeast reveal templated insertions and strand-specific insertion/deletion profiles. Proc Natl Acad Sci USA. 2018;115(9):E2040-E2047. doi:10.1073/pnas.1716855115.

Liang Z, Sunder S, Nallasivam S, Wilson TE. Overhang polarity of chromosomal double-strand breaks impacts kinetics and fidelity of yeast non-homologous end joining. Nucleic Acids Res. 2016;44(6):2769–2781. doi:10.1093/nar/gkw013.

Llorente B, Symington LS. The Mre11 nuclease is not required for 5′ to 3′ resection at multiple HO-induced double-strand breaks. Mol Cell Biol. 2004;24(21):9682–9694. doi:10.1128/MCB.24.21.9682-9694.2004.

Ma JL, Kim EM, Haber JE, Lee SE. Yeast Mre11 and Rad1 proteins define a Ku-independent mechanism to repair double-strand breaks lacking overlapping end sequences. Mol Cell Biol. 2003;23(23):8820–8828. doi:10.1128/MCB.23.23.8820-8828.2003.

Mimitou EP, Symington LS. Sae2, Exo1 and Sgs1 collaborate in DNA double-strand break processing. Nature. 2008;455(7214):770–774. doi:10.1038/nature07312.

Moreau S, Ferguson JR, Symington LS. The nuclease activity of Mre11 is required for meiosis but not for mating type switching, end joining, or telomere maintenance. Mol Cell Biol. 1999;19(1):556–566. doi:10.1128/MCB.19.1.556.

Nitiss KC, Malik M, He X, White SW, Nitiss JL. Tyrosyl-DNA phosphodiesterase (Tdp1) participates in the repair of Top2-mediated DNA damage. Proc Natl Acad Sci USA. 2006;103(24):8953–8958. doi:10.1073/pnas.0603455103.

Paques F, Haber JE. Two pathways for removal of nonhomologous DNA ends during double-strand break repair in *Saccharomyces cerevisiae*. Mol Cell Biol. 1997;17(11):6765–6771. doi:10.1128/MCB.17.11.6765.

Pouliot JJ, Yao KC, Robertson CA, Nash HA. Yeast gene for a Tyr-DNA phosphodiesterase that repairs topoisomerase I complexes. Science. 1999;286(5439):552–555. doi:10.1126/science.286.5439.552.

Reginato G, Cejka P. The MRE11 complex: a versatile toolkit for the repair of broken DNA. DNA Repair (Amst). 2020;91–92:102869. doi:10.1016/j.dnarep.2020.102869.

Schwartz EK, Heyer WD. Processing of joint molecule intermediates by structure-selective endonucleases during homologous recombination in eukaryotes. Chromosoma. 2011;120(2):109–127. doi:10.1007/s00412-010-0304-7.

Sfeir A, Symington LS. Microhomology-mediated end joining: a back-up survival mechanism or dedicated pathway? Trends Biochem Sci. 2015;40(11):701–714. doi:10.1016/j.tibs.2015.08.006.

Shaltz S, Jinks-Robertson S. Mutagenic repair of a ZFN-induced double-strand break in yeast: effects of cleavage site sequence and spacer size. DNA Repair (Amst). 2021;108:103228. doi:10.1016/j.dnarep.2021.103228.

Symington LS. Mechanism and regulation of DNA end resection in eukaryotes. Crit Rev Biochem Mol Biol. 2016;51(3):195–212. doi:10.3109/10409238.2016.1172552.

Symington LS, Rothstein R, Lisby M. Mechanisms and regulation of mitotic recombination in *Saccharomyces cerevisiae*. Genetics. 2014;198(3):795–835. doi:10.1534/genetics.114.166140.

Teo SH, Jackson SP. Identification of *Saccharomyces cerevisiae* DNA ligase IV: involvement in DNA double-strand break repair. EMBO J. 1997;16(15):4788–4795. doi:10.1093/emboj/16.15.4788.

Tseng SF, Gabriel A, Teng SC. Proofreading activity of DNA polymerase Pol2 mediates 3′-end processing during nonhomologous end joining in yeast. PLoS Genet. 2008;4(4):e1000060. doi:10.1371/journal.pgen.1000060.

Tseng HM, Tomkinson AE. A physical and functional interaction between yeast Pol4 and Dnl4-Lif1 links DNA synthesis and ligation in nonhomologous end joining. J Biol Chem. 2002;277(47):45630–-45637. doi:10.1074/jbc.M206861200.

Villarreal DD, Lee K, Deem A, Shim EY, Malkova A, Lee SE. Microhomology directs diverse DNA break repair pathways and chromosomal translocations. PLoS Genet. 2012;8(11):e1003026. doi:10.1371/journal.pgen.1003026.

Westmoreland JW, Resnick MA. Coincident resection at both ends of random, γ-induced double-strand breaks requires MRX (MRN), Sae2 (Ctp1), and Mre11-nuclease. PLoS Genet. 2013;9(3):e1003420. doi:10.1371/journal.pgen.1003420.

Wilson TE, Lieber MR. Efficient processing of DNA ends during yeast nonhomologous end joining. Evidence for a DNA polymerase beta (Pol4)-dependent pathway. J Biol Chem. 1999;274(33):23599–-23609. doi:10.1074/jbc.274.33.23599.

Xu G, Chapman JR, Brandsma I, Yuan J, Mistrik M, Bouwman P, Bartkova J, Gogola E, Warmerdam D, Barazas M, *et al.* REV7 counteracts DNA double-strand break resection and affects PARP inhibition. Nature. 2015;521(7553):541–544. doi:10.1038/nature14328.

Zhang X, Paull TT. The Mre11/Rad50/Xrs2 complex and non-homologous end-joining of incompatible ends in *S. cerevisiae*. DNA Repair (Amst). 2005;4(11):1281–1294. doi:10.1016/j.dnarep.2005.06.011.

Editor: J. Surtees